

Biophysical Journal, Volume 111

Supplemental Information

Voltage Dependence of Conformational Dynamics and Subconducting States of VDAC-1

Rodolfo Briones, Conrad Weichbrodt, Licia Paltrinieri, Ingo Mey, Saskia Villinger, Karin Giller, Adam Lange, Markus Zweckstetter, Christian Griesinger, Stefan Becker, Claudia Steinem, and Bert L. de Groot

Voltage dependence of conformational dynamics and
sub-conducting states of VDAC-1.

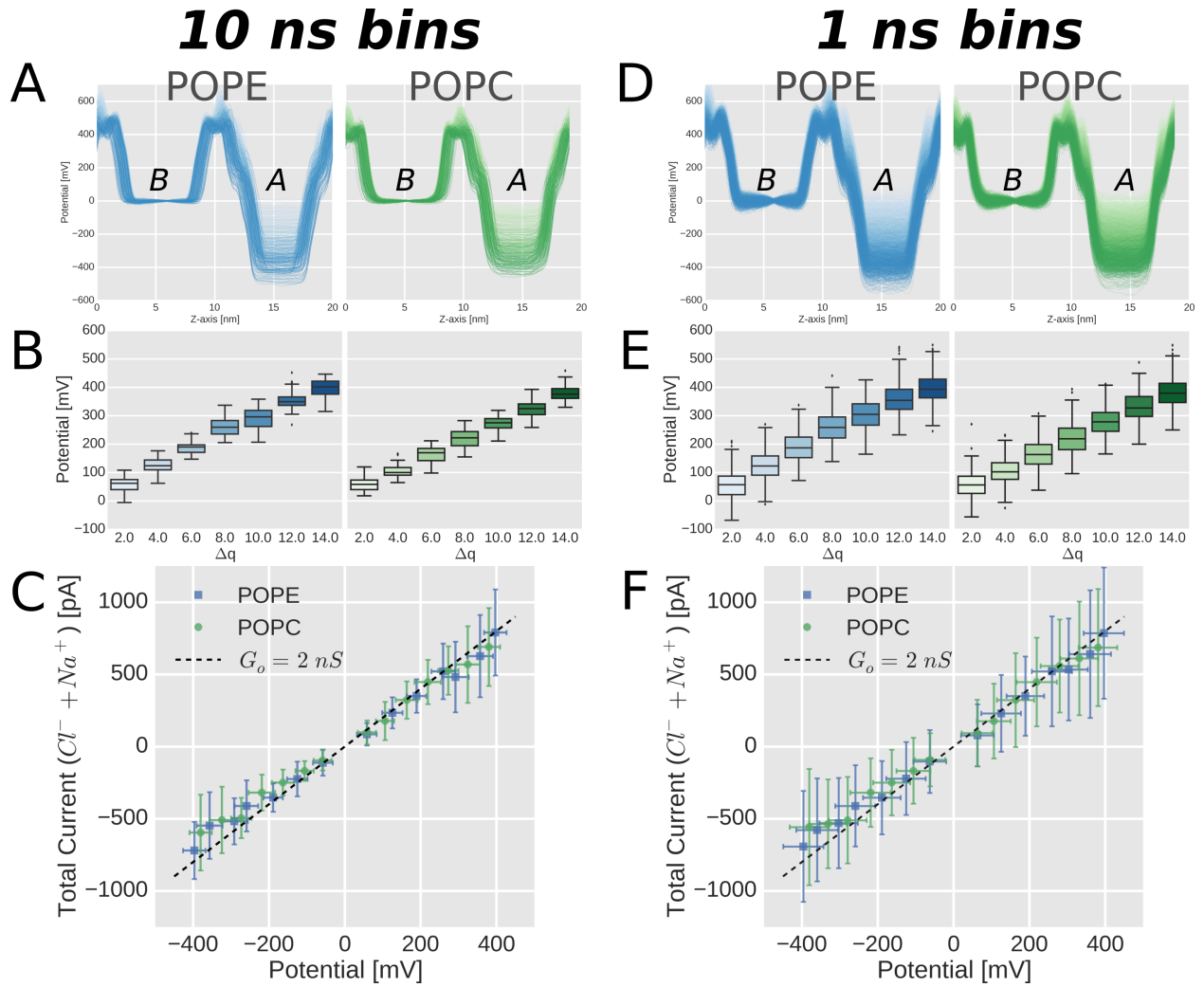
SUPPORTING MATERIAL

R. Briones, C. Weichbrodt, L. Paltrinieri,
I. Mey, S. Villinger, K. Giller,
A. Lange, M. Zweckstetter, C. Griesinger,
S. Becker, C. Steinem, and B. L. de Groot

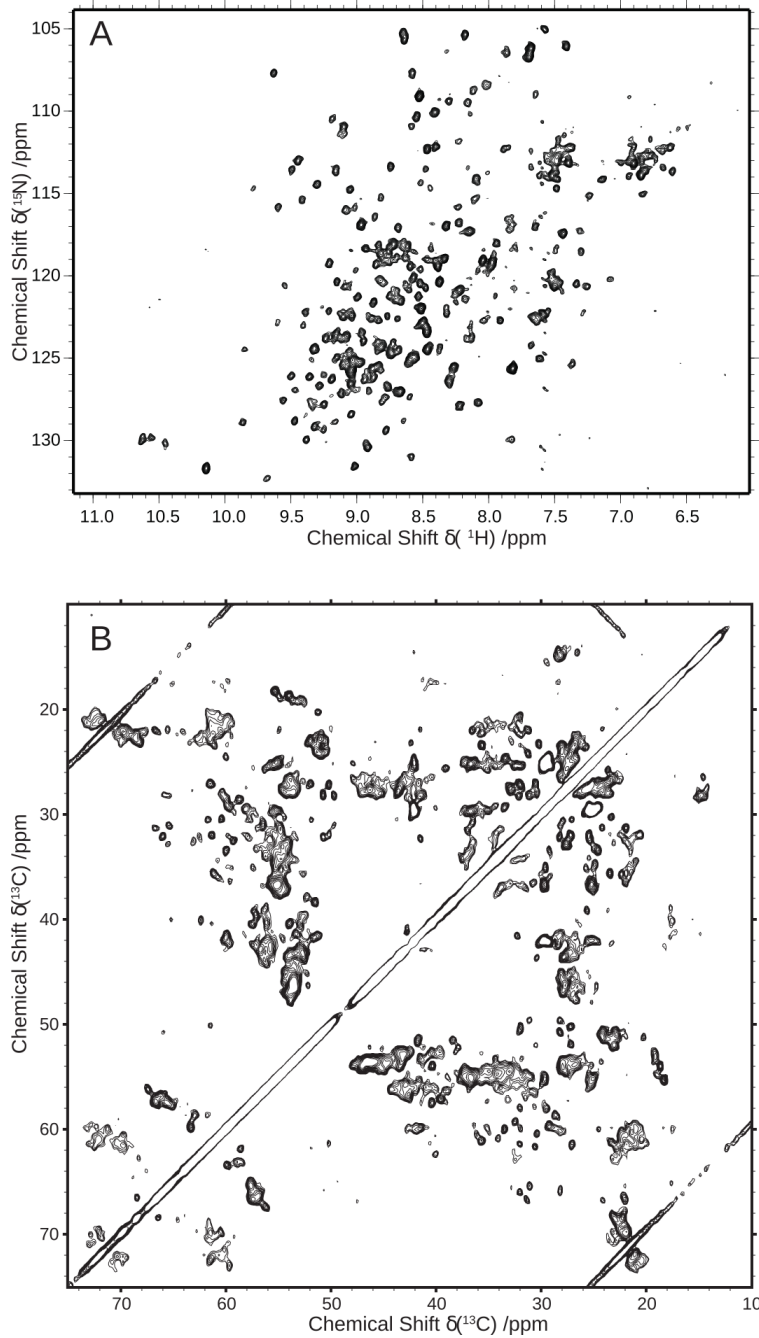
July 17, 2016

References

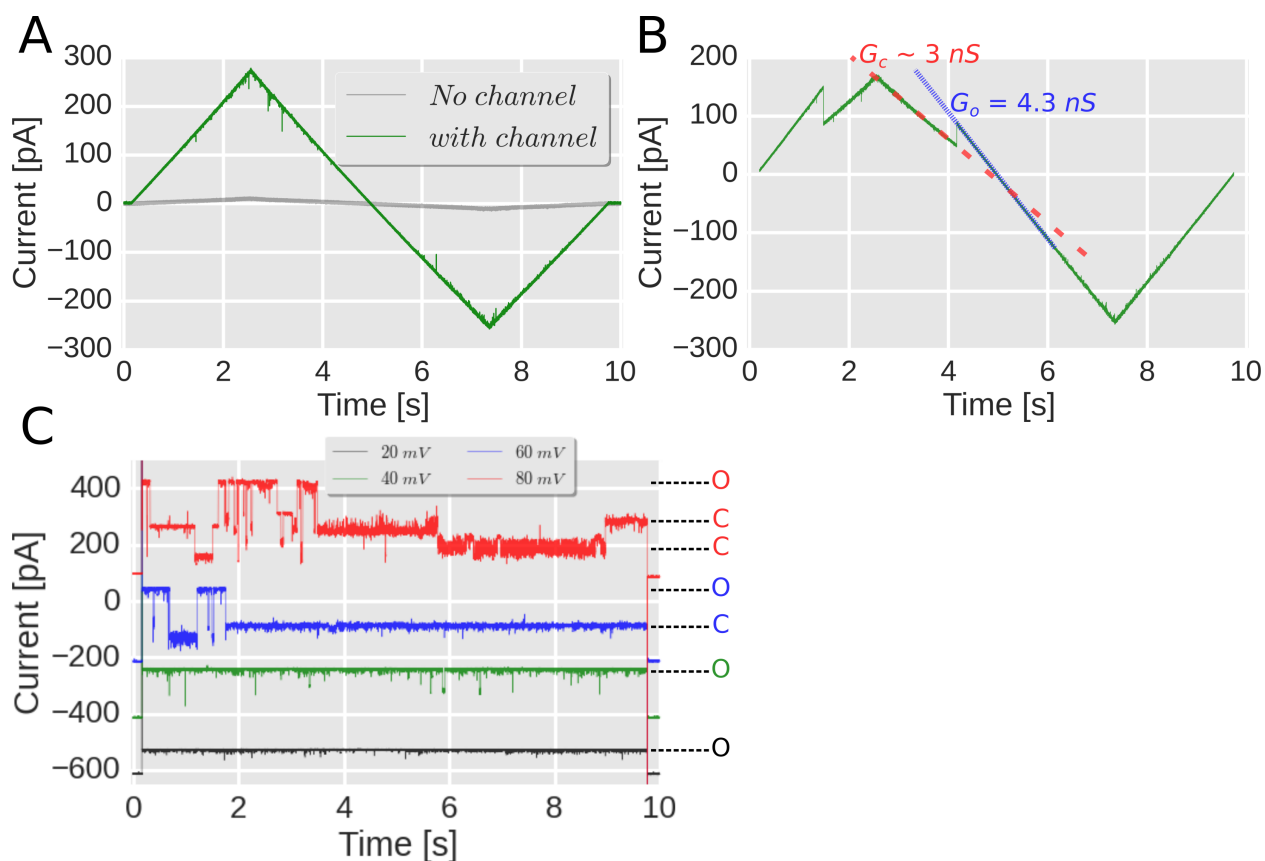
1. Paramo, T., A. East, D. Garzón, M. B. Ulmschneider, and P. J. Bond, 2014. Efficient Characterization of Protein Cavities within Molecular Simulation Trajectories: *trj_cavity*. *J Chem Theory Comput* 10:2151–2164.



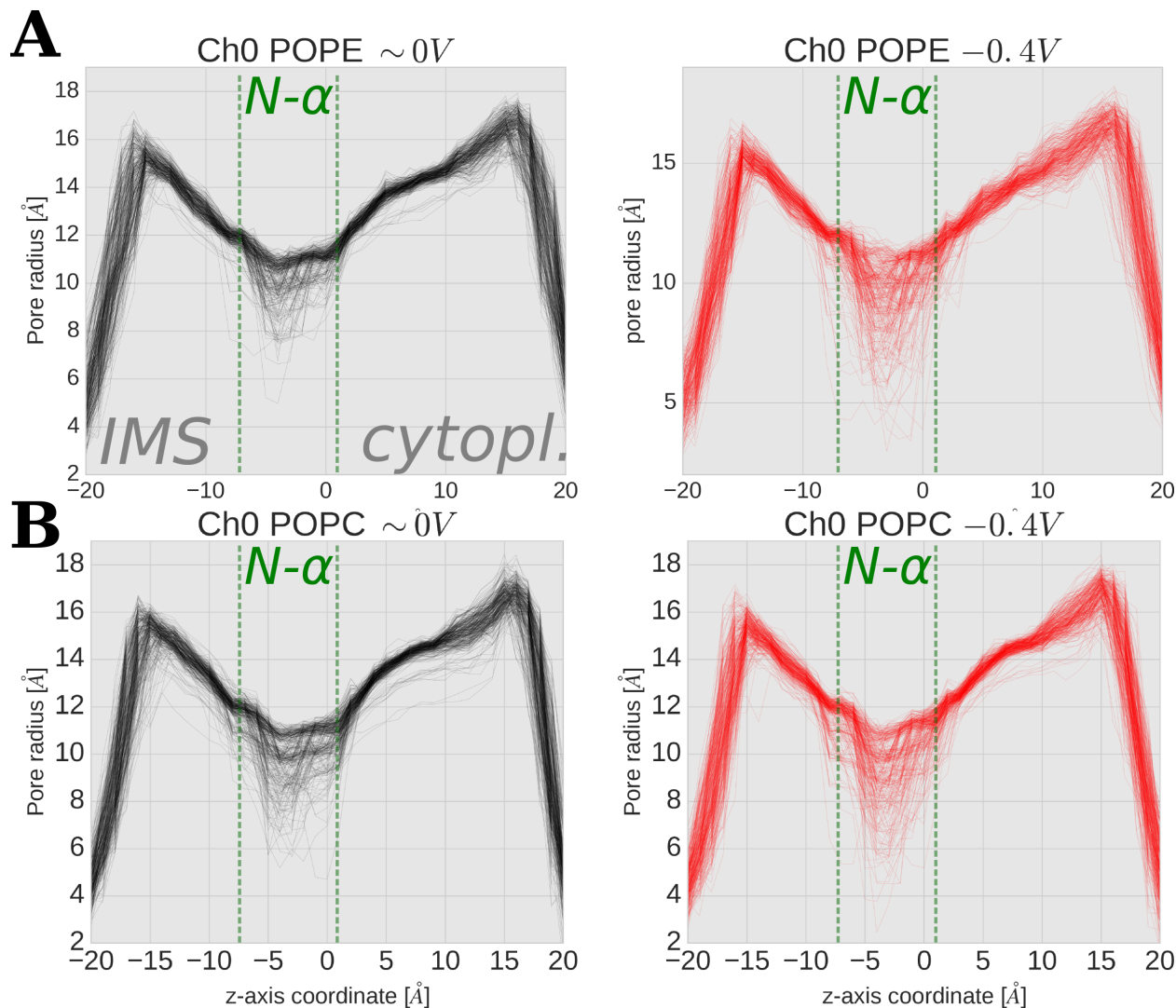
Supplementary Figure S1: **Binning effect on the electrostatic potential and current-voltage (I/V) relationship.** **A** and **D** show the potentials across the z -axis of the double bilayer systems. Labels *A* and *B* indicate the solution region of compartments, where time-averaged potential differences (ΔV) were calculated using either 10 or 1 *ns* window bins. The curves of POPE and POPC systems for all Δq are shown. Δq increases from 2 to 14 charges and it is shown from *pale blue* to *blue* for POPE, and from *pale green* to *green* for POPC. **B** and **E** show the ΔV distribution (quartile box-plots) between compartments *A* and *B* as a function of Δq for POPE and POPC, respectively. **C** and **F** show the I/V relationships for POPE and POPC. The symbols and crosses depict mean and standard deviations. The experimental ‘open’ VDAC conductance of 2 *nS* at 0.5 M *NaCl* is shown as a *black* segmented line. The mean conductance values ($\pm SEM$) for the negative (\ominus) and positive (\oplus) voltages were the following: For the 10 *ns* bins: \ominus 1.63 (± 0.08) and \oplus 1.96 (± 0.11) *nS* in POPE, and \ominus 1.56 (± 0.08) and \oplus 1.92 (± 0.10) *nS* in POPC. For the 1 *ns* bins: \ominus 1.62 (± 0.05) and \oplus 1.94 (± 0.06) *nS* in POPE, and \ominus 1.58 (± 0.05) and \oplus 1.89 (± 0.06) *nS* in POPC.



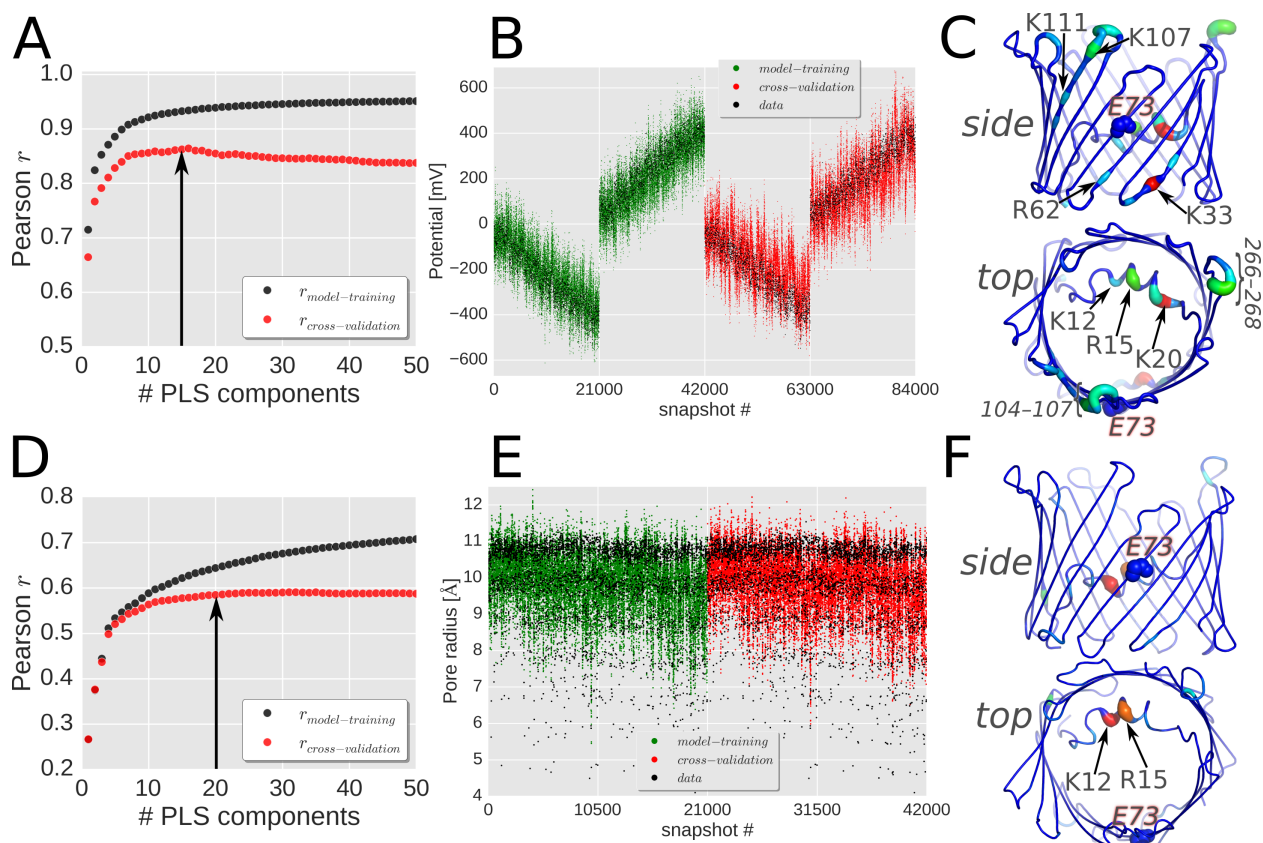
Supplementary Figure S2: NMR spectra of wild-type hVDAC-1. A. ^1H , ^{15}N -TROSY spectrum of wild-type hVDAC-1 in LDAO. B. ^{13}C - ^{13}C proton-driven spin diffusion (PDSO) solid-state NMR spectra of wild-type hVDAC-1 in DMPC liposomes, demonstrating the structural integrity of the protein.



Supplementary Figure S3: **Experimental electrophysiology traces at 1 M KCl.** **A.** Current response of a DPhPC/cholesterol membrane with and without an inserted hVDAC-1. A voltage-ramp with a frequency of 100 mHz and an amplitude of $\pm 60 \text{ mV}$ was applied. Without the protein, a conductance of 0.042 nS is found. In the presence of a single hVDAC-1 a conductance in the range from 4 to 4.5 nS was obtained. **B.** Current response of a DPhPC/cholesterol membrane with a single hVDAC-1 inserted. The voltage-ramp protocol is the same as in **A**. At larger potentials the channel closes and opens again as indicated by the stepwise drop and rise in current, resulting in a change in conductance from a value of $4\text{--}4.5 \text{ nS}$ (G_o blue segmented line) to a value of below 3 nS (G_c red segmented line). **C.** Voltage-clamp current traces of a DPhPC/cholesterol membrane with a single hVDAC-1 inserted. Traces of 10 s were measured at 20 mV (black), 40 mV (green), 60 mV (blue), and 80 mV (red). At constant lower potentials, the channel remains mostly in the ‘open’ state (O). At larger potentials, the channel ‘closes’ (C), visiting several less conductive states.



Supplementary Figure S4: **Pore radius profiles of VDAC at negative Voltages.** The `trj_cavity` software (1) was used to calculate the pore radius profiles. The found pores covered a region of ~ 32 Å, spanning the IMS (negative z) and cytoplasmatic (positive z) sides of the pore. The $z = 0$ correspond to the center of mass of the protein. The location of $N\text{-}\alpha$ is marked by the green segmented lines. **A** Pore radius profiles of mVDAC-1 simulated in POPE lipids. A constant ion difference of $2q$ translated in an average voltage estimate of ~ 0 V, left (black lines). A constant ion difference of $14q$ translated in an average voltage estimate of ~ -0.4 V, right (red lines). **B** Pore radius profiles of mVDAC-1 simulated in POPC lipids. A constant ion difference of $2q$ translated in an average voltage estimate of ~ 0 V, left (black lines). A constant ion difference of $14q$ translated in an average voltage estimate of ~ -0.4 V, right (red lines). The narrower region of the pore profile coincides with the location of $N\text{-}\alpha$.



Supplementary Figure S5: **PLS-FMA conformational models cross-validation and amino acid contribution to fluctuations.** The models were constructed using the time-averaged voltage (1 ns) of VDAC simulations and the instantaneous minimal pore radius (min_r), these values were correlated with the structures of the protein without hydrogens, which correspond to 2171 atoms. Half of the data was used for model-training and the other half for cross-validation. **A–C** PLS-FMA information for the voltage conformational model. 84000 frames were used in total. **A** shows that the Pearson correlation coefficient converges at 15 components (*black arrow*). **B**. Original data, model-training (mVDAC-1 in PE lipids) and cross-validation part (mVDAC-1 in PC lipids) of the 15 components conformational model. **C**. The RMSF (root mean squared fluctuation) of the amino acids in the conformational model. This indicates the amino acids which fluctuate the most along the voltage conformational model. Colors closer to red in a *BGR* color scale, and broader tube widths indicate more mobile amino acids. The location of E73 in the barrel is indicated by the blue spheres. **D–F** PLS-FMA information for the min_r *ch0*. 42000 frames were used in total. **D** shows that the Pearson correlation coefficient converges at 20 components (*black arrow*). **E**. Original data, model-training and cross-validation part of the 20 components conformational model. **F**. The RMSF (root mean squared fluctuation) of the amino acids in the conformational model. This indicates the amino acids which fluctuate the most along the min_r conformational model. Colors closer to red in a *BGR* color scale (*blue-green-red*), and broader tube widths indicate more mobile amino acids. The location of E73 in the barrel is indicated by the blue spheres.

Table S1. Forces and Electric field acting on KRK and R218 aas.

Δq (potential)	ChX (polarity)	K20		R15		K12		R218	
		Total	Electrost.	Total	Electrost.	Total	Electrost.	Total	Electrost.
Forces [kJ mol ⁻¹ nm ⁻¹]									
0 (-0 V)	0 (-)	-18.4 (±750)	-238.9 (±404.8)	0.5 (±536.6)	-82.8 (±358.6)	-19.9 (±614.2)	-88.6 (±337.7)	16.7 (±550.5)	56.8 (±295.8)
0	1 (+)	15.0 (±807.4)	-170.3 (±394.3)	1.4 (±523.1)	-101.4 (±416.5)	9.2 (±651.3)	-60.8 (±408.1)	11.7 (±556.9)	149.0 (±335.8)
14 (-0.4 V)	0 (-)	-4.5 (±614.3)	428.3 (±444.1)	5.4 (±555.8)	257.8 (±332.8)	12.8 (±591.3)	-68.9 (±391.4)	-0.9 (±557.1)	154.2 (±342.3)
14 (+0.4 V)	1 (+)	-19.6 (±786.6)	-270.0 (±407.5)	-0.1 (±554.3)	-207.1 (±374.3)	-6.3 (±628.9)	-207.9 (±371.0)	-12.7 (±592.3)	42.5 (±319.1)
[V nm ⁻¹]									
0 (-0 V)	0 (-)	-0.2	-2.5	0	-0.9	-0.2	-0.9	0.2	0.6
0	1 (+)	0.2	-1.8	0	-1.1	0.1	-0.6	0.1	1.5
14 (-0.4 V)	0 (-)	0	4.4	0.1	2.7	0.1	-0.7	0	1.6
14 (+0.4 V)	1 (+)	-0.2	-2.8	0	-2.1	-0.1	-2.2	-0.1	0.4

Average forces and field were calculated on the COM of the side-chain atoms.

Table S2. Salt bridging analysis of selected positive mVDAC-1 amino acids

Δq	Chx(polarity)	K20			R15			K12			R218		
		P(sb)	partners	Mean-Z-N+ (±SD) [Å]	P(sb)	partners	Mean-Z-N+ (±SD)	P(sb)	partners	Mean-Z-N+ (±SD)	P(sb)	partners	Mean-Z-N+ (±SD)
2	0 (-)	0.39	D16, E280	-5.6 (±1.9)	0.04	D16, D9	0.6 (±1.9)	0.42	D16, D9	-6.3 (±1.3)	0.90	E189	12.1 (±1.3)
2	1 (+)	0.40	D16, E280	-6.0 (±1.8)	0.12	D16, D9	-0.6 (±1.5)	0.38	D16, D9	-6.9 (±1.3)	0.90	E189	12.4 (±1.2)
8	0	0.13	D16	-4.3 (±2.4)	0.01	D16, D9, E189	1.2 (±2.0)	0.41	D16, D9	-5.7 (±1.6)	0.77	E189	12.6 (±1.7)
8	1	0.26	D16, E203, E280	-6.8 (±1.6)	0.14	D16, D9	-0.8 (±1.6)	0.38	D16, D9	-7.3 (±1.2)	0.86	E189	12.4 (±1.1)
14	0	0.21	D16	-0.0 (±3.2)	0.04	D16, E189	2.5 (±2.1)	0.40	D16, D9	-5.1 (±1.8)	0.62	E189	13.6 (±2.0)
14	1	0.32	D16, E203	-7.7 (±1.4)	0.21	D16, D9	-1.3 (±1.7)	0.29	D16, D9	-7.8 (±1.3)	0.82	E189	12.4 (±1.4)

Δq	Chx(polarity)	R120			K109			K53			K113		
		P(sb)	partners	Mean-Z-N+ (±SD)	P(sb)	partners	Mean-Z-N+ (±SD)	P(sb)	partners	Mean-Z-N+ (±SD)	P(sb)	partners	Mean-Z-N+ (±SD)
2	0 (-)	0.98	E121	-16.1 (±0.8)	0.43	D132	16.4 (±2.0)	0.18	D78	14.3 (±2.1)	0.28	D100, D128, D130, D132	8.0 (±1.2)
2	1 (+)	0.74	E121	-15.9 (±1.1)	0.47	D132	17.3 (±2.0)	0.14	D78	14.3 (±2.0)	0.27	D100, D128, D130, D132	7.6 (±1.2)
8	0	0.90	E121	-16.1 (±0.8)	0.54	D132	15.8 (±2.1)	0.14	D78	14.3 (±2.0)	0.30	D100, D128, D130, D132	8.6 (±1.3)
8	1	0.75	E121	-15.9 (±0.9)	0.69	D132	16.4 (±1.9)	0.15	D78	14.5 (±2.0)	0.39	D100, D128, D130	7.3 (±0.9)
14	0	0.99	E121	-15.9 (±0.8)	0.30	D132	16.2 (±2.0)	0.12	D78	14.6 (±2.0)	0.39	D100, D128, D130, D132	8.9 (±1.1)
14	1	0.68	E121	-15.7 (±1.0)	0.49	D132	16.6 (±1.9)	0.45	D78	13.1 (±2.0)	0.27	D100, D128, D130, D132	7.2 (±1.1)

P(sb) is defined by the proportion of $N_{\text{H}}-O_{\text{H}}$ distances below 4.5 Å.

Mean-Z-N+ defines the mean Z-coordinate (±SD) of the side-chain nitrogens. Zero correspond to the Protein COM, IMS values in the negative, and cytosolic positive. 10 replicas, 30 ns each were used for each ion difference (Δq) and channel polarity Chx (Ch0 (-) and Ch1 (+)).